American Mineralogist, Volume 77, pages 558–564, 1992

Experimental determination of the reaction 2magnetite + 2kyanite + 4quartz = 2almandine + O_2 at high pressure on the magnetite-hematite buffer

DANIEL E. HARLOV
Department of Earth and Atmospheric Sciences, Purdue University, West Lafayette, Indiana 47907, U.S.A.
ROBERT C. NEWTON
Department of the Geophysical Sciences, The University of Chicago, 5734 South Ellis Avenue, Chicago, Illinois 60637, U.S.A.

ABSTRACT

The equilibrium almandine + kyanite + magnetite + quartz + O_2 buffered to magnetite + hematite f_{O_2} has been reversed at corresponding temperatures and pressures of 650 °C and 21.5 kbar, 700 °C and 22.25 kbar, 800 °C and 25.75 kbar, and 900 °C and 28.5 kbar. A new buffering technique was used that can hold an experiment at magnetite + hematite f_{O_2} at 800 °C and 26 kbar for periods of up to 5 d. The reversed brackets may be fitted with thermodynamic data for the phases tabulated by Berman (1988, 1990) if his enthalpy of formation for almandine is revised to -5272.00 ± 0.40 kJ/mol at 298 K. Use of this enthalpy in calculating the position of the almandine + rutile + sillimanite + ilmenite + quartz and almandine + sillimanite + hercynite + quartz equilibria in turn requires the enthalpy of formation for ilmenite and hercynite to be -1234.2 and -1955.1 kJ/mol, respectively, at 298 K and 1 bar. The assemblage almandine + kyanite + magnetite + quartz can serve as an O barometer in high-grade rocks, such as granulites, where the temperature and pressure of recrystallization are independently known.

INTRODUCTION

Almandine garnet is an important phase in the estimation of regional metamorphic pressures and temperatures. Because of its high density compared to other chemically equivalent mineral assemblages, almandine figures prominently in a variety of geobarometers derived from experimentally reversed equilibria. Examples of pressure-sensitive assemblages include almandine + rutile + sillimanite + ilmenite + quartz (GRAIL) (Bohlen et al., 1983a), almandine + grossular + fayalite + anorthite (Bohlen et al., 1983b), almandine + grossular + ferrosilite + anorthite + quartz (Bohlen et al., 1980, 1983b; Perkins and Chipera, 1985), almandine + sillimanite + hercynite + quartz (Bohlen et al., 1986), and almandine + grossular + rutile + ilmenite + anorthite + quartz (Bohlen and Liotta, 1986). In addition almandine-pyrope solutions exhibit a relatively large Fe-Mg distribution coefficient (K_d) with minerals such as olivine (Hackler and Wood, 1989), orthopyroxene (Lee and Ganguly, 1988), biotite (Ferry and Spear, 1978), and clinopyroxene (Pattison and Newton, 1989), which facilitates its use in K_d exchange thermometers.

Despite its widespread use, the enthalpy of formation for almandine garnet is still relatively uncertain. Chatillon-Colinet et al. (1983), using high-temperature solution calorimetry with an oxide melt [$(Li,Na)BO_2$] of almandine, fayalite, corundum, and quartz at 750 °C, determined an enthalpy of formation for almandine of -5270.81 ± 5.73 kJ/mol at 298 K. Woodland and Wood (1989) have measured electrochemically a ΔG_f for almandine between 1073 and 1173 K using the equilibrium $2Fe + \frac{2}{3}Al_2SiO_5 + \frac{4}{3}SiO_2 + O_2 = \frac{2}{3}Fe_3Al_2Si_3O_{12}$ by measuring the f_{O_2} of this reaction relative to quartz + fayalite + Fe at 1 bar. They then used the Berman (1988) data set to calculate a ΔH_f for almandine of -5267.8 kJ/mol. The veracity of their result is somewhat in question, however, since there is considerable difficulty in actually performing this reaction at atmospheric pressure as evidenced, in part, by our own results (Table 1). In contrast, experimental phase equilibria, particularly GRAIL (e.g., Holland and Powell, 1990; Berman, 1988; Anovitz and Essene, 1987), have also been used to determine enthalpies of formation for almandine with thermochemical data for the other minerals taken from measured and derived sources. These almandine enthalpies are as much as 7 kJ/mol less negative than the calorimetric value.

In this study we have reversed the equilibrium

$$\underset{\text{magnetite}}{2Fe_3O_4} + \underset{\text{kyanite}}{2Al_2SiO_5} + \underset{\text{quartz}}{4SiO_2} = \underset{\text{almandine}}{2Fe_3Al_2Si_3O_{12}} + O_2 \quad (1)$$

buffered to magnetite + hematite f_{O_2},

$$\underset{\text{hematite}}{6Fe_2O_3} = \underset{\text{magnetite}}{4Fe_3O_4} + O_2 \quad (2)$$

at high temperatures and pressures.

We have determined values of ΔG_f and ΔH_f for almandine from the experimental brackets. Our value for the almandine enthalpy of formation is in turn used to calculate a ΔH_f value for hercynite from the reversals of almandine + sillimanite + hercynite + quartz of Bohlen

0003–004X/92/0506–0558$02.00

TABLE 1. Experimental results

Experiment	T (°C)	P (kbar)	Time (h)	Cylinder (in.)	Results
90-AM-22	650	23	168	1	*Alm* Mt Ky Qtz
90-AM-26	650	20	240	1	Alm *Mt Ky Qtz*
90-AM-23	700	28	72	¾	*Alm* (Mt Ky Qtz)
90-AM-24	700	25	60	¾	*Alm* (Mt Ky Qtz)
90-AM-25	700	22	72	¾	Alm *Mt Ky Qtz*
90-AM-31	700	23.5	132	¾	*Alm* Mt Ky Qtz
90-AM-32	700	23	168	¾	*Alm* Mt Ky Qtz
90-AM-35	700	22.5	132	¾	*Alm* Mt Ky Qtz
90-AM-42	700	22	144	¾	Alm *Mt Ky Qtz*
90-AM-19	800	10.5	73	1	(Alm) *Mt Ky Qtz*
90-AM-20	800	15	46	1	(Alm) *Mt Ky Qtz*
90-AM-21	800	20	23	1	(Alm) *Mt Ky Qtz*
90-AM-27	800	27	44	¾	*Alm* Mt Ky Qtz
90-AM-28	800	25	45	¾	(Alm) *Mt Ky Qtz*
90-AM-29	800	26	45	¾	*Alm* Mt Ky Qtz
90-AM-30	800	25.5	91	¾	Alm *Mt Ky Qtz*
90-AM-33	850	10	48	¾	(Alm) *Mt Ky Qtz*
90-AM-37	900	28	36	¾	Alm *Mt Ky Qtz*
90-AM-41	900	29	48	¾	*Alm* Mt Ky Qtz
90-AM-46	900	30	36	¾	*Alm* Mt Ky Qtz

Note: The italicized phases indicate a relative increase in peak height of 15–20% over the other phases. Parentheses indicate that the phase either totally disappeared or only remained in trace amounts.

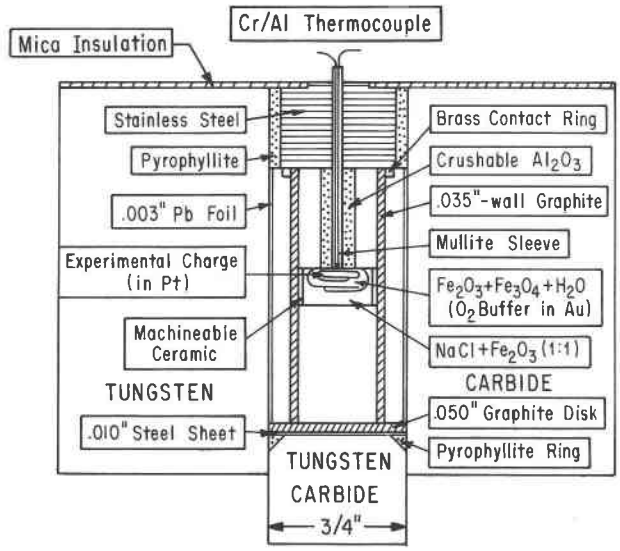

Fig. 1. Scale drawing of the modified NaCl-graphite furnace assembly for the ¾-in.-diameter piston cylinder showing the location of the large Au capsule, Fe_2O_3-NaCl packing, and ceramic shield. Unlabeled parts within the assembly consist of pressed and dried NaCl.

et al. (1986) and a ΔH_f value for ilmenite from the GRAIL equilibrium of Bohlen et al. (1983a). Standard thermodynamic properties of the substances in Equilibria 1 and 2, including all heat capacity and volumetric data, were taken from the data set of Berman (1988, 1990).

EXPERIMENTAL METHOD

The experiments were performed in a ¾-in. and a 1-in. piston-cylinder apparatus using a low temperature NaCl-graphite furnace assembly as described in Bohlen (1984), with some modifications (Fig. 1). These included a large-bore graphite furnace (½-in. diameter) to allow for the insertion of large Au capsules (4-mm diameter) with relatively little distortion.

For experiments at 650, 700, and 800 °C, 10-mg charges, consisting of almandine, magnetite, quartz, and kyanite in reaction proportions plus 2 mg of H_2O, were loaded into Pt capsules, which were sealed by arc welding. For experiments at 900 °C, 10 mg of the almandine + kyanite + magnetite + quartz mix plus 5 mg of hematite and 0.5 mg of H_2O were loaded into the Pt capsule. The Pt capsule, plus 100 mg of Fe_2O_3 and 10 mg of H_2O, were packed into a large Au capsule, which was also sealed by arc welding.

The inner Pt capsule served as a membrane across which H_2 was maintained in equilibrium between the inner and outer capsules. This in turn allowed equilibration of the partial pressure of O_2 as well. That the f_{O_2} was at the magnetite-hematite buffer both within and outside the Pt capsule was evidenced by the partial oxidation of magnetite to hematite within the Pt capsule and the partial reduction of hematite to magnetite within the large Au capsule. According to calculations presented by Ganguly and Newton (1968), depletion of Fe in the charge by the Pt capsule is negligible in a system buffered to magnetite + hematite f_{O_2}.

The immediate area around the large Au capsule was packed with an equal-weight mixture of Fe_2O_3 and NaCl in order to help maintain the magnetite-hematite buffer in the capsule. The mixture was shielded from the graphite furnace by a thin-walled ceramic cylinder (Fig. 1). This was done because, in earlier unshielded experiments, hematite reducing to magnetite on the inner surface of the graphite furnace results in localized melting of the salt, probably due to the generation of CO_2. The ceramic shield also served to keep the Au capsule from coming in contact with the graphite furnace.

The ceramic sheathed chromel-alumel thermocouple was situated such that the tip, coated with a thin layer of Al_2O_3 cement, rested directly atop the large Au capsule (Fig. 1). The overall accuracy of the thermocouple, including temperature gradients within the setup, accuracy of the controller, and the accuracy of the chromel-alumel thermocouple (with no correction for pressure), is estimated to be within ±10 °C of the actual temperature. We used the piston-out technique by elevating the pressure to a point approximately 20% below the desired pressure and then increasing the temperature to experimental conditions. The thermal expansion of the salt took the experiment up to the final pressure. We observed no anomalous behavior in the salt expansion, despite the presence of the 50/50 Fe_2O_3/NaCl mix in the immediate area of the Au capsule. Total uncertainty in the pressure, including both calibration and pressure fluctuation, is estimated to be ±0.2 kbar with no correction for friction. No difference in either the pressure calibration or uncertainty was seen among the three presses used nor between the

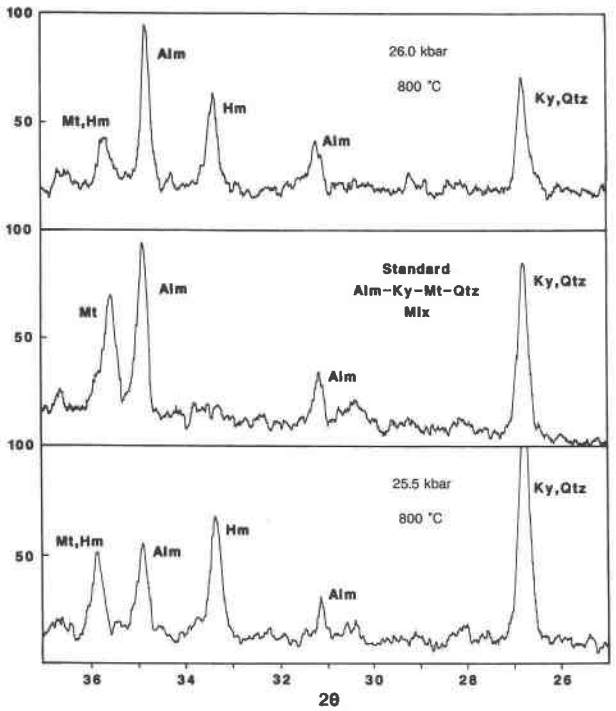

Fig. 2. Comparison of powder diffraction X-ray spectra of the charge before and after experiments at 26 and 25.5 kbar at 800 °C. The experiment at 26 kbar shows almandine growth with respect to magnetite, kyanite, and quartz and a prominent hematite peak. The experiment at 25.5 kbar shows growth of kyanite, magnetite, and quartz with respect to almandine. Again a prominent hematite peak has appeared.

1-in. and ¾-in. pressure assemblies. The duration of the experiments ranged from 12 h to 10 d. During the experiment both pressure and the current through the graphite furnace were carefully monitored. The experiments reported in Table 1 are those in which the capsule seals held, in which the magnetite-hematite buffer was maintained, in which there was no significant shift in pressure or current through the graphite furnace, and in which there was no disruption in the experimental NaCl-graphite furnace setup such as would have been caused by localized melting of the pressure medium or faulting in the graphite furnace.

Characterization of starting material and experimental products

A natural quartz from Lisbon, Maryland (General Chemical Corporation), was crushed to <0.1 mm grain size, leached with dilute HF + H_2SO_4, and ignited. Remaining non-quartz impurities were stated to be less than 0.03 wt%. Blades of a pale blue natural kyanite, hand picked from a polycrystalline aggregate of unknown locality (University of Chicago, Department of the Geophysical Sciences Collection no. 4959) and free of sheet silicate, were crushed to a powder (<0.1 mm). Subsequent mounting of this powder in refractive index oil (n = 1.540) showed no microscopically visible foreign phases. Microprobe analysis indicated an Fe_2O_3 content of 0.1 oxide wt% on average. Semieuhedral crystals of magnetite from an anorthosite in Quebec were crushed to less than a 0.1-mm grain size. Microprobe analysis indicated an Al_2O_3 content of approximately 0.5 oxide wt%, on average, with no other minor components.

Almandine garnet was grown in 150-mg batches from a finely crushed almandine glass plus 10 mg of H_2O placed in large Au capsules, arc-welded shut, and then subjected to pressures and temperatures of 28 kbar and 1000 °C for periods of 24–48 h, using the ¾-in. piston-cylinder apparatus and NaCl-graphite furnace assembly. The glass, Alak 5, was made by Andrea Koziol using techniques outlined in Koziol and Newton (1989) and in Geiger et al. (1987).

Relative growth or decrease of a mineral phase by 15–20% was determined using powder X-ray diffraction spectra of the charges. The heights of pairs of closely spaced, prominent X-ray peaks were compared with respect to the ratio of their heights in the original mix. Figure 2 shows X-ray spectra for the 800 °C charges at pressures of 25.5 and 26.0 kbar, along with that of the standard mix. From the relative peak heights, growth of almandine relative to magnetite and kyanite + quartz is evident at 26 kbar, whereas the opposite is true at 25.5 kbar. These results were confirmed, in part, by examination of a small portion of each experiment mounted in refractive index oil (n = 1.540) under a cover slip, as well as through reproducibility of X-ray spectra. Large growth or decline of product or reactant assemblages was usually evidenced by abundance changes in the mount.

In addition to the growth or decrease of phases, successful experiments were also characterized by the oxi-

Table 2. Analyses of synthetic products of equilibrium experiments

	Almandine				Kyanite				Magnetite			
	90-AM-22		90-AM-28		90-AM-30		90-AM-27		90-AM-31		90-AM-37	
SiO_2	35.03	(2.924)	34.40	(2.882)	36.24	(0.987)	36.67	(0.989)	0.00	(0.000)	0.00	(0.000)
Al_2O_3	20.22	(1.990)	21.20	(2.094)	60.19	(1.933)	60.93	(1.937)	0.62	(0.028)	0.06	(0.003)
Fe_2O_3	2.57	(0.161)	2.26	(0.142)	4.06	(0.083)	3.82	(0.078)	67.71	(1.972)	68.07	(1.997)
FeO	41.88	(2.924)	41.13	(2.882)	0.00	(0.000)	0.00	(0.000)	30.90	(1.000)	30.66	(1.000)
Total	99.70		98.99		100.49		101.42		99.23		98.79	

Note: Microprobe analyses were performed on a Cameca SX50 microprobe with a beam current of 15 nA and accelerating voltage of 15 kV. Standards consisted of synthetic fayalite, magnetite, and corundum and natural kyanite and pyrope.

dation of a portion of the magnetite to hematite within the Pt capsule such that the experimental product always contained coexisting magnetite and hematite (Fig. 2). Hematite was conspicuous in the oil mounts as dark red euhedral to semieuhedral hexagonal plates. This fact ensured that the experimental product indeed had been buffered to magnetite + hematite f_{O_2}. The presence of magnetite was further confirmed using a magnet.

High resolution X-ray powder diffraction patterns of the product almandine from four of the experiments with an internal standard (high purity corundum annealed at 1350 °C for 48 h) yielded a mean unit-cell parameter a_o of 11.5353 ± 0.0003 Å (1σ). This unit-cell parameter corresponds, by means of the linear interpolation described in Geiger et al. (1987), to an almandine garnet that contains approximately 5.0 ± 0.5 mol% of the Fe^{3+} end-member skiagite, i.e., $(Fe^{2+})_3(Fe^{3+})_2Si_3O_{12}$, with an assumed error range of ±0.001 Å. Similar X-ray powder diffraction patterns of three samples of the starting almandine, when the same internal standard is used, indicate an identical a_o of 11.5351 ± 0.0007 Å (1σ). The Fe^{3+} estimates derived from a_o agree very well with Fe^{3+} values determined from microprobe analyses of starting and final almandine, which indicate a skiagite component in the range of 4–6 mol% (Table 2). Representative microprobe analyses of product almandine, magnetite, and kyanite, given in Table 2, show little difference from their starting material counterparts, with the exception of product kyanite, which has increased markedly in Fe_2O_3.

Results and thermodynamic considerations

Equilibrium 1 was experimentally reversed at 650, 700, 800, and 900 °C (Fig. 3, Table 1). At 700 and 800 °C the reversals are within 500 bars, which provide tight constraints on the dP/dT slope of the reaction. For comparison, calculation of the stability of almandine + kyanite + magnetite + quartz buffered to magnetite + hematite f_{O_2} may be carried out with the use of a self-consistent data set, in this case that of Berman (1990) for almandine and Berman (1988) for the remaining phases, by the relationship

$$\Delta G(P,T) = \Delta H(P,T) - T(\mathrm{K})\Delta S(P,T) + \mathrm{R}T \ln K\alpha + \mathrm{R}T \ln f_{O_2} = 0 \qquad (3)$$

where ΔG, ΔH, and ΔS are, respectively, the Gibbs free energy, enthalpy, and entropy changes of the reaction with stoichiometric phases, $K\alpha$ is an activity ratio that allows for the effects of any nonstoichiometry, f_{O_2} is the fugacity of oxygen, and R is the ideal gas constant. Taken together, $K\alpha$ and f_{O_2} make up the equilibrium coefficient K_{eq}.

The resulting equilibrium in P-T space (Fig. 3) lies approximately 3 kbar above our reversals, indicating that some of the tabulated thermodynamic properties, probably the enthalpy for one or more of the phases, is incorrect. Of the phases in Equilibria 1 and 2, the thermochemical data for quartz and O_2 are well established (Holland and Powell, 1990; Berman, 1988; Robie et al., 1978). For kyanite, heat capacity data, accurately determined by Robie and Hemingway (1984), are incorporated in the Berman (1988) data set. The enthalpy of formation of kyanite is also well determined by the experimentally reversed equilibrium kyanite + corundum + quartz (Peterson and Newton, 1990). Their enthalpy agrees well with Berman's tabulated value. Berman (1988) based his enthalpy data for magnetite and hematite on the experimental work of Myers and Eugster (1983), taking his C_P data from sources also used by Holland and Powell (1990) and Robie et al. (1978). Heat capacities for all these phases have been experimentally determined over a wide range of temperatures.

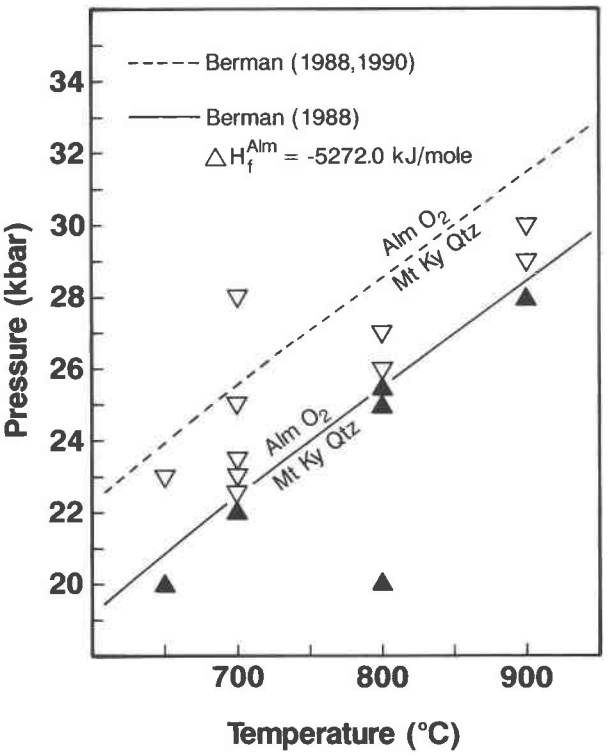

Fig. 3. Plot of experimental reversals. The equilibrium predicted by the Berman (1988) data set, with the almandine enthalpy and entropy taken from Berman (1990), is plotted with the same equilibrium calculated using our value (−5272.0 kJ/mol) for the almandine enthalpy of formation. Open and filled triangles indicate growth of the high-pressure and low-pressure assemblages, respectively.

In contrast, thermochemical data for almandine is more uncertain. The heat capacity and standard entropy of almandine have been measured at low temperatures (420–997 K) by adiabatic and differential scanning calorimetry (cf. Berman, 1988, 1990; Anovitz and Essene, 1987). These heat capacities, along with their extrapolated values at higher temperatures, are incorporated in Berman's data base. With the exception of one relatively uncertain (±6 kJ/mol) calorimetric study (Chatillon-Colinet et al., 1983) (Table 3), the enthalpy of formation of almandine is generally found from equilibria with other minerals (Berman, 1988, 1990; Holland and Powell, 1990).

TABLE 3. Enthalpies of formation (298 K, 1 bar) kJ/mol

Almandine	Ilmenite	Hercynite	Reference
	−1236.62	−1966.48	Robie et al. (1978)
−5270.81 ± 5.73			Chatillon-Colinet et al. (1983)
−5263.78	−1230.45		Anovitz and Essene (1987)
−5265.50	−1231.95		Berman (1988)
−5267.8			Woodland and Wood (1989)
−5267.22			Berman (1990)
−5267.85	−1233.26	−1956.00	Holland and Powell (1990)
		−1947.68	Sack and Ghiorso (1991)
−5272.00 ± 0.40	−1234.16	−1955.11	this study

A rigorous determination of the almandine enthalpy consistent with the reversals presented in this study and with those considered by Berman (1990) would essentially involve a reevaluation of many of the noncalorimetric enthalpies within the data base, especially those associated with equilibria containing almandine, magnetite, and hematite, using the techniques outlined by Berman (1988). In this study we choose, as a first approximation, to adjust only the almandine enthalpy. We find that if this enthalpy is made 4.8 kJ/mol more negative (−5272.00 kJ/mol) than the value given in Berman (1990) (−5267.2 kJ/mol), the almandine + kyanite + magnetite + quartz equilibrium is shifted downward such that it now fits quite snugly between the reversals (Fig. 3).

The tight brackets at 700 and 800 °C place effective constraints on the slope of the equilibrium. In Figure 3, the slope defined by the brackets agrees well with the slope of the equilibrium determined using the Berman (1988) data base and our value for the almandine enthalpy, which lends support to the validity of the calorimetric entropy, C_P, and volume data of the mineral phases, especially almandine, tabulated by Berman (1988). The uncertainty interval (±0.25 kbar) of these two brackets translates into an error range of ±0.40 kJ/mol for our value of the almandine enthalpy, which is compared in Table 3 with previously published values.

In calculating the position of the equilibrium in *P-T* space, the net effect of the mixing due to minor components such as Fe^{3+} in almandine, Al in magnetite, and Fe^{3+} in kyanite was found to be minor and within the error range of the pressure for the reversals at 700 and 800 °C. In the case of almandine and kyanite, this mixing was assumed to be ideal, whereas in the case of magnetite, the spinel mixing model of Sack and Ghiorso (1991) was used. Microprobe analyses of the hematite found it to be without any minor components.

MINERALOGICAL APPLICATIONS

Application of our value for the almandine enthalpy to other experimentally determined equilibria, including the almandine + rutile + sillimanite + ilmenite + quartz (GRAIL) equilibrium (Bohlen et al., 1983a) and the almandine + sillimanite + hercynite + quartz equilibrium (Bohlen et al., 1986) requires additional departures from the Berman (1988) data set. In order to fit the experimental brackets, the enthalpy of one or more of the other phases must be adjusted. For the almandine + rutile + sillimanite + ilmenite + quartz equilibrium (Bohlen et al., 1983a), the ilmenite enthalpy is, after almandine, the most uncertain parameter. Adjusting the enthalpy of ilmenite to a value 2 kJ/mol more negative (−1234.2 kJ/mol) than the value given by Berman (1988) (−1231.95 kJ/mol) shifts the equilibrium upward to fit the reversals (Fig. 4). Our self-consistent value for the ΔH_f of ilmenite is almost exactly midway between the Berman (1988) value and that tabulated by Robie et al. (1978) (−1236.6 kJ/mol) (Table 3). While both data sets derive their ilmenite enthalpy from the same experimental studies, the Berman data set follows the derivations of Anovitz et al. (1985).

The principle unknown in the almandine + sillimanite + hercynite + quartz equilibrium (Bohlen et al., 1986) after almandine is hercynite. Using our value for the almandine enthalpy of formation and assigning a value of −1955.1 kJ/mol for the hercynite enthalpy of formation gives a relatively good fit to the reversals (Fig. 4). Cation ordering, deviations from R_3O_4 stoichiometry, and substitution of Fe_3O_4 are not considered in arriving at this estimate (cf. Sack and Ghiorso, 1991). Entropy and heat capacity data for hercynite used in the calculations are taken from Sack and Ghiorso (1991). Our ΔH_f value is in good agreement with Holland and Powell (1990) and lies approximately halfway between the values given by Robie et al. (1978) and Sack and Ghiorso (1991) (Table 3). Mössbauer studies of the starting synthetic hercynite by Bohlen et al. (1986) indicated a magnetite component of approximately 2%. The cell dimensions of the hercynite were found to be the same before and after the experiment, which would seem to conclude that little if any additional Fe^{3+} had substituted into the hercynite. In this study, the hercynite was treated as end-member hercynite in all calculations.

Equilibrium 1, the oxidation of almandine, constitutes an intrinsic O barometer for rocks bearing the requisite assemblage, provided that the temperature and pressure of recrystallization are independently known. It would be necessary to know accurately the free energy of mixing of garnet components other than almandine; comprehensive mixing models such as that of Berman (1990) or Ganguly and Saxena (1984) may be used. In addition it is probable that the magnetite will have an ulvospinel component, for which mixing properties are described in Andersen et al. (1991) or Sack and Ghiorso (1991). Com-

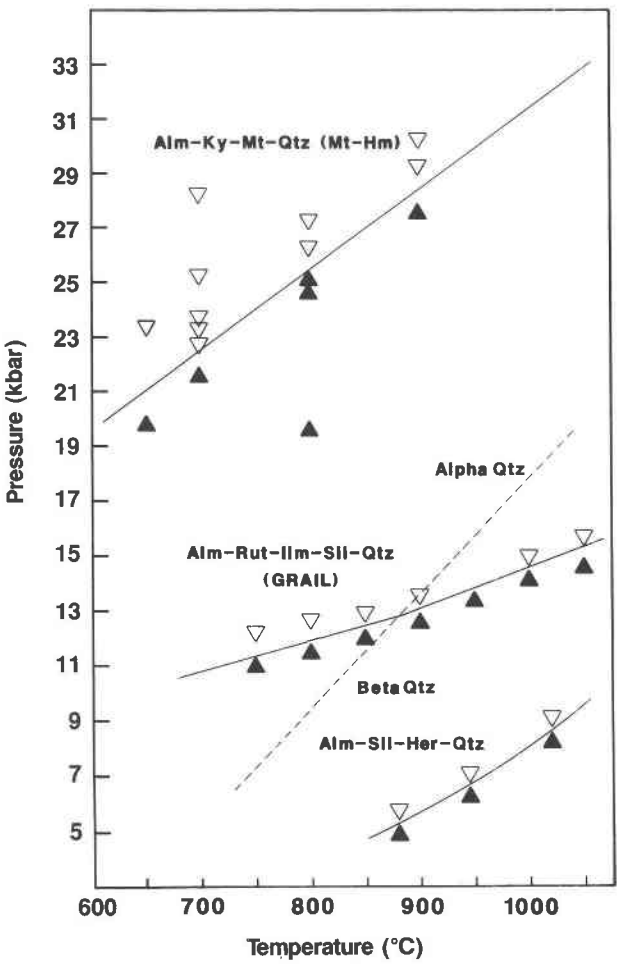

Fig. 4. Plot of reversals and equilibria for almandine + kyanite + magnetite + quartz buffered to magnetite + hematite f_{O_2}, almandine + rutile + sillimanite + ilmenite + quartz (Bohlen et al., 1983a), and almandine + sillimanite + hercynite + quartz (Bohlen et al., 1986). The equilibria were recalculated using the almandine, ilmenite, and hercynite enthalpies determined in this study. All other thermodynamic data are taken from the Berman (1988) data set. Open and filled triangles indicate stability of the high-pressure and low-pressure assemblages, respectively.

parison may be made, and internal consistency sought, with other oxybarometer assemblages that may exist in the rock, such as titaniferous magnetite + ilmenite (Andersen et al., 1991; Ghiorso and Sack, 1991), quartz + titanomagnetite + ilmenite + olivine (QUILF; Frost et al., 1988), and quartz + titanomagnetite + ilmenite + orthopyroxene (QUILP; Peterson, 1989; Lindsley et al., 1990).

The almandine oxidation equilibrium buffered at magnetite-hematite also offers the possibility of measuring the free energy of solid solution with Fe^{2+} of other garnet constituents such as Mg or Mn, inasmuch as these will stabilize the garnet to lower pressures than for pure almandine. This lowering in pressure acts as a direct measure of the almandine activity.

Acknowledgments

This research was supported by a U.S. National Science Foundation grant, no. 9015581 (R.C.N.). Additional support was provided by the Materials Research Laboratory (NSF) at the University of Chicago.

References cited

Andersen, D.J., Bishop, F.C., and Lindsley, D.H. (1991) Internally consistent solution models for Fe-Mg-Mn-Ti oxides: Fe-Mg-Ti oxides and olivine. American Mineralogist, 76, 427–444.

Anovitz, L.M., and Essene, E.J. (1987) Compatibility of geobarometers in the system CaO-FeO-Al_2O_3-SiO_2-TiO_2 (CFAST): Implications for garnet mixing models. Journal of Geology, 95, 633–645.

Anovitz, L.M., Treiman, A.H., Essene, E.J., Hemingway, B.S., Westrum, E.F., Wall, V.J., Burriel, R., and Bohlen, S.R. (1985) The heat-capacity of ilmenite and phase equilibria in the system Fe-Ti-O. Geochimica et Cosmochimica Acta, 49, 2027–2040.

Berman, R.G. (1988) Internally-consistent thermodynamic data for minerals in the system Na_2O-K_2O-CaO-MgO-FeO-Fe_2O_3-Al_2O_3-SiO_2-TiO_2-H_2O-CO_2. Journal of Petrology, 29, 445–522.

——— (1990) Mixing properties of Ca-Mg-Fe-Mn garnets. American Mineralogist, 75, 328–344.

Bohlen, S.R. (1984) Equilibria for precise pressure calibration of a frictionless furnace assembly of the piston-cylinder apparatus. Neues Jahrbuch für Mineralogie Monatshefte, 1, 404–412.

Bohlen, S.R., and Liotta, J.J. (1986) A barometer for garnet amphibolites and garnet granulites. Journal of Petrology, 27, 1025–1034.

Bohlen, S.R., Essene, E.J., and Boettcher, A.L. (1980) Reinvestigation and application of olivine-quartz-orthopyroxene barometry. Earth and Planetary Science Letters, 47, 1–10.

Bohlen, S.R., Wall, V.J., and Boettcher, A.L. (1983a) Experimental investigations and geological applications of equilibria in the system FeO-TiO_2-Al_2O_3-SiO_2-H_2O. American Mineralogist, 68, 1049–1058.

——— (1983b) Experimental investigation and application of garnet granulite equilibria. Contributions to Mineralogy and Petrology, 83, 52–61.

Bohlen, S.R., Dollase, W.A., and Wall, V.J. (1986) Calibration and applications of spinel equilibria in the system FeO-Al_2O_3-SiO_2. Journal of Petrology, 27, 1143–1156.

Chatillon-Colinet, C., Kleppa, O.J., Newton, R.C., and Perkins, D. (1983) Enthalpy of formation of $Fe_3Al_2Si_3O_{12}$ (almandine) by high temperature alkali borate solution calorimetry. Geochimica et Cosmochimica Acta, 47, 439–444.

Ferry, J.M., and Spear, F.S. (1978) Experimental calibration of the partitioning of Fe and Mg between biotite and garnet. Contributions to Mineralogy and Petrology, 66, 113–117.

Frost, B.R., Lindsley, D.H., and Andersen, D.J. (1988) Fe-Ti oxide-silicate equilibria: Assemblages with fayalitic olivine. American Mineralogist, 73, 727–740.

Ganguly, J., and Newton, R.C. (1968) Thermal stability of chloritoid at high pressure and relatively high oxygen fugacity. Journal of Petrology, 9, 444–466.

Ganguly, J., and Saxena, S.K. (1984) Mixing properties of aluminosilicate garnets: Constraints from natural and experimental data, and applications to geothermobarometry. American Mineralogist, 69, 88–97.

Geiger, C.A., Newton, R.C., and Kleppa, O.J. (1987) Enthalpy of mixing of synthetic almandine-grossular and almandine-pyrope garnets from high-temperature solution calorimetry. Geochimica et Cosmochimica Acta, 51, 1755–1763.

Ghiorso, M.S., and Sack, R.O. (1991) Fe-Ti oxide geothermometry: Thermodynamic formulation and the estimation of intensive variables in silicic magmas. Contributions to Mineralogy and Petrology, 108, 485–510.

Hackler, R.T., and Wood, B.J. (1989) Experimental determination of Fe and Mg exchange between garnet and olivine and estimation of Fe-Mg mixing properties in garnet. American Mineralogist, 74, 994–999.

Holland, T.J.B., and Powell, R. (1990) An enlarged and updated consis-

tent thermodynamic dataset with uncertainties and correlations: The system K_2O-Na_2O-CaO-MgO-MnO-FeO-Fe_2O_3-Al_2O_3-TiO_2-SiO_2-C-H_2-O_2. Journal of Metamorphic Geology, 8, 89–124.

Koziol, A.M., and Newton, R.C. (1989) Grossular activity-composition relationships in ternary garnets determined by reversed displaced-equilibrium experiments. Contributions to Mineralogy and Petrology, 103, 423–433.

Lee, H.Y., and Ganguly, J. (1988) Equilibrium compositions of coexisting garnet and orthopyroxene: Experimental determinations in the system FeO-MgO-Al_2O_3-SiO_2. Journal of Petrology, 29, 93–113.

Lindsley, D.H., Frost, B.R., Andersen, D.J., and Davidson, P.M. (1990) Fe-Ti oxide-silicate equilibria: Assemblages with orthopyroxene. In R.J. Spencer and I.-M. Chou, Eds., Fluid-mineral interactions: A tribute to H.P. Eugster, p. 103–119. Pergamon Press, New York.

Myers, J., and Eugster, H.P. (1983) The system Fe-Si-O: Oxygen buffer calibrations to 1500 K. Contributions to Mineralogy and Petrology, 82, 75–90.

Pattison, D.R.M., and Newton, R.C. (1989) Reversed experimental calibration of the garnet-clinopyroxene Fe-Mg exchange thermometer. Contributions to Mineralogy and Petrology, 101, 87–103.

Perkins, D., and Chipera, S.J. (1985) Garnet-orthopyroxene-plagioclase-quartz barometry: Refinement and application to the English River Subprovince and the Minnesota River Valley. Contributions to Mineralogy and Petrology, 89, 69–80.

Peterson, D.E. (1989) Estimation of the QUILP equilibrium. Eos, 70, 493–494.

Peterson, D.E., and Newton, R.C. (1990) Free energy and enthalpy of formation of kyanite. Geological Society of America Abstracts with Program, 22, 342.

Robie, R.A., and Hemingway, B.S. (1984) Entropies of kyanite, andalusite, and sillimanite: Additional constraints on the pressure and temperature of the Al_2SiO_5 triple point. American Mineralogist, 69, 298–306.

Robie, R.A., Hemingway, B.S., and Fisher, J.R. (1978) Thermodynamic properties of minerals and related substances at 298.15 K and 1 bar (10^5 pascals) pressure and at higher temperatures. U.S. Geological Survey Bulletin 1452, 456 p.

Sack, R.O., and Ghiorso, M.S. (1991) Chromian spinels as petrogenetic indicators: Thermodynamics and a petrologic application. American Mineralogist, 76, 827–847.

Woodland, A.B., and Wood, B.J. (1989) Electrochemical measurement of the free energy of almandine ($Fe_3Al_2Si_3O_{12}$) garnet. Geochimica et Cosmochimica Acta, 53, 2277–2282.

Manuscript received July 8, 1991
Manuscript accepted January 13, 1992